JTTEE5 15:811-816
DOI: 10.1361/105996306X147162
1059-9630/$19.00 © ASM International

Characterizations and Hot Corrosion Resistance of Cr_3C_2-NiCr Coating on Ni-Base Superalloys in an Aggressive Environment

T.S. Sidhu, S. Prakash, and R.D. Agrawal

(Submitted April 2, 2006; in revised form July 2, 2006)

In the current study, Cr_3C_2-NiCr coating was deposited on the Ni-base superalloys by using high velocity oxyfuel (HVOF) process for high temperature corrosive environment applications. Optical microscopy (OM), x-ray diffraction (XRD), scanning electron microscopy/energy-dispersive analysis (SEM/EDAX), microhardness tester, and electro probe microanalyzer (EPMA) techniques were used to characterize the coating with regard to coating thickness, porosity, microhardness, and microstructure. The thermogravimetric technique was used to establish kinetics of corrosion. The hot corrosion behaviors of the bare and Cr_3C_2-NiCr coated superalloys were studied after exposure to aggressive environment of Na_2SO_4-60%V_2O_5 salt mixture at 900 °C under cyclic conditions. The structure of the as-sprayed Cr_3C_2-NiCr coating mainly consisted of γ-nickel solid solution along with minor phases of Cr_7C_3 and Cr_2O_3. Coating has porosity less than 1.5% and microhardness in the range of 850-900 Hv (Vickers hardness). Some inclusions, unmelted and semimelted powder particles were observed in the structure of the coatings. The Cr_3C_2-NiCr coating has imparted necessary resistance to hot corrosion, which has been attributed to the formation of oxides of nickel and chromium, and spinel of nickel-chromium.

Keywords Cr_3C_2-NiCr, high velocity oxyfuel, hot corrosion, Ni-Based superalloys, protective coating

1. Introduction

High velocity oxyfuel (HVOF) process is a relatively new and rapidly developing technology, which can produce dense coatings with high hardness and adhesion values, and good erosion, corrosion, and wear resistance properties (Ref 1). This process has been widely adopted by many industries due to its flexibility and cost effectiveness.

Hot corrosion is a serious problem in boilers, gas turbines, internal combustion engines, and industrial waste incinerators. It consumes the materials at an unpredictably rapid rate. As a consequence the load-carrying abilities of the components are reduced, leading eventually to their catastrophic failure (Ref 2). Vanadium, sodium, and sulphur are the common impurities in low-grade petroleum fuels. Molten sulphate-vanadate deposits resulting from the condensation of combustion products of such fuels are extremely corrosive to high temperature materials in combustion systems (Ref 3). A mixture of Na_2SO_4 and V_2O_5 in the ratio of 40:60 constitutes a eutectic with a low melting point of 550 °C and provides a very aggressive environment for hot corrosion to occur (Ref 4). Further, cyclic study provides the severest conditions for testing. It represents the actual industrial conditions where breakdown/shutdown occurs frequently. Thermally sprayed (Cr_xC_y-NiCr) coatings can be used for higher temperature applications in light of the excellent corrosion and oxidation resistance of the nickel chromium alloy and reasonable wear resistance of the chromium carbides at temperatures up to 900 °C (Ref 5).

The present research work is aimed to characterize the HVOF sprayed Cr_3C_2-NiCr coating on Ni-based superalloys and to evaluate their performance in an aggressive environment of Na_2SO_4-60%V_2O_5 salt mixture at 900 °C under cyclic conditions. The superalloys selected for this study have been provided by Mishra Dhatu Nigam Limited, Hyderabad (India) and are used in boilers and gas turbines applications. The coating has been characterized with respect to microstructure, porosity, microhardness, and phase formation using the combined techniques of optical microscopy (OM), x-ray diffraction (XRD), scanning electron microscopy/energy-dispersive analysis (SEM/EDAX), and electro probe micro analyzer (EPMA).

2. Experimental Procedure

2.1 Substrate Materials and Coating Powder

The Ni-base superalloys, namely Superni 75 (19.5Cr-3Fe-0.3Ti-0.1C-balance Ni) and Superni 601 (23Cr-12.35Fe-1.48Al-0.8Mn-0.37Si-0.10Cu-0.025C-balance Ni) (wt.%) were used as substrate materials for this study. A commercially available Cr_3C_2-NiCr powder (LA-6875, blend of 75%LA-6304 and 25% LA-7319) of nominal composition of 75%Cr_3C_2-25%(Ni-20Cr) (wt.%) and particle size of −325 mesh (< 44 μm) was used in this study. SEM of the powder (Fig. 1) shows that the

This article was originally published in *Building on 100 Years of Success, Proceedings of the 2006 International Thermal Spray Conference* (Seattle, WA), May 15-18, 2006, B.R. Marple, M.M. Hyland, Y.-Ch. Lau, R.S. Lima, and J. Voyer, Ed., ASM International, Materials Park, OH, 2006.

T.S. Sidhu, S. Prakash, and **R.D. Agrawal,** Metallurgical and Materials Engineering Department, Indian Institute of Technology Roorkee, Roorkee-247667 (UA) India. Contact e-mail: tssidhu@rediffmail.com.

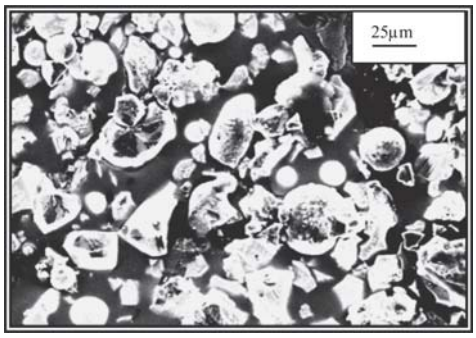

Fig. 1 SEM of Cr_3C_2-NiC powder

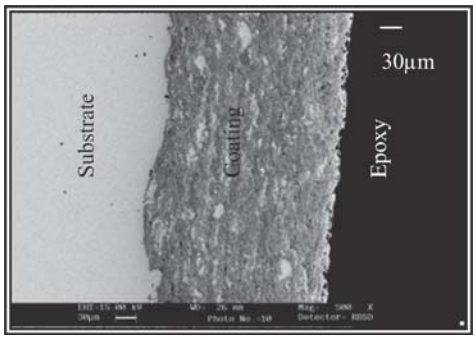

Fig. 2 BSE image of as-sprayed Cr_3C_2-NiC coating

powder consists of Cr_3C_2 irregularly shaped particles and Ni-20%Cr spherical particles. The bigger particles have a size less than 44 μm, consistent with the nominal size distribution provided by the manufacturer (Lineage Alloys, Baytown, TX)

2.2 Deposition and Characterization of the Coatings

Coating was sprayed at M/S Metallizing Equipment Co. Pvt. Ltd., Jodhpur (India) with a Hipojet-2100 HVOF System (Metal Spray Suppliers Ltd., New Zealand), using liquefied petroleum gas (LPG) as a fuel. The spray parameters used for Hipojet-2100 system were oxygen flow rate, 250 LPM; fuel (LPG) flow rate, 60 LPM; airflow rate, 900 LPM; spray distance, about 20 cm; fuel pressure, 6 kg/cm^2; oxygen pressure, 8 kg/cm^2; air pressure, 6 kg/cm^2. The details for specimen preparations, spray parameters, and equipment/instruments used for characterization of the coating/corrosion products have been reported in the earlier publications of the authors (Ref 6-8).

2.3 Molten Salt Corrosion Tests

Cyclic studies were performed in molten salt (Na_2SO_4-60%V_2O_5) for 50 cycles. Each cycle consisted of 1 h heating at 900 °C in a silicon carbide tube furnace followed by 20 min cooling at room temperature. The studies were performed for uncoated as well as coated specimens for the purpose of comparison. The specimens were mirror polished down to 1 μm alumina wheel cloth polishing before corrosion run. Thereafter, the specimens were washed with acetone and heated in an oven to about 250 °C. The specimens were heated to ensure proper adhesion of the salt layer. A layer of Na_2SO_4-60%V_2O_5 mixture prepared in distilled water was applied uniformly on the warm specimens with the help of a camel hairbrush. Amount of the salt coating was kept in the range of 3.0-5.0 mg/cm^2. The salt-coated specimens as well as the alumina boats were then kept in the oven for 3-4 h at 100 °C. Then they were again weighed before exposing to hot corrosion tests in the tube furnace. The salt mixture was applied on the surface only once in the beginning of the test and it was not replenished during the test. During hot corrosion runs, the weight of boats and specimens were measured together at the end of each cycle with the help of Electronic Balance Machine Model 06,120 (Contech, Mumbai, India) with a sensitivity of 1 mg. The spalled scale was also included at the time of measurements of weight change to determine total rate of corrosion.

3. Results and Discussions

Cr_3C_2-NiCr coating was deposited successfully by HVOF technique on Ni-base superalloys using LPG as fuel gas. The thickness of the coating as measured from the backscattered electron (BSE) images (Fig. 2) was found to be in the desired range of 200-250 μm, thereby ensuring integrity of the coating. Higher thickness may lead to disintegration of the coatings due to the presence of residual stresses.

3.1 Porosity

Porosity is one of the most important properties of the coatings for higher temperature applications in corrosive environments, as porosities are the preferential corrosion paths through which the corrosive species can penetrate the coatings to reach the substrate and may cause rapid corrosion attack. Dense coatings usually provide better corrosion resistance than porous coatings (Ref 9). Porosity or voids in the coating microstructure is an important issue in thermal spraying, as due to this physical property corrosion resistance of different thermal spraying coatings differs. The porosity in the current study has been identified by a PMP3 inverted metallurgical microscope made in Japan with stereographic imaging, and image analyzer with Dewinter Material Plus 1.01 software based on ASTM B276 (Ref 10) was used to determine the porosity values. The porosity of the coatings has been found to be less than 1.5%. The low value of porosity might be due to high kinetic energy of the powder particles. In the HVOF process, the powder particles are propelled out of the gun nozzle at high velocities toward the substrate. Due to the high velocity impact of the sprayed powder particles, there may be an excellent joining of flat disc particles with the substrate and with an interlayer, and thus the coatings produced by HVOF spraying process are very dense. The measured values of the porosity are in close agreement with the findings of Guilemany et al. (Ref 11) and Suegama et al. (Ref 12).

3.2 Microhardness

In many aggressive environments, protective coatings may have to encounter the problems of erosion-corrosion degradation. The softer coatings are more susceptible to erosion-corrosion mode of degradation. The microhardness profiles

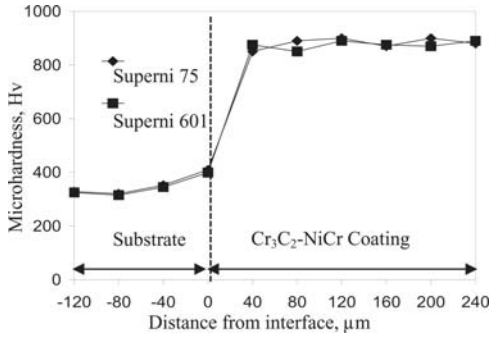

Fig. 3 Microhardness profiles of HVOF sprayed Cr_3C_2-NiCr coating for different superalloys along the cross section

along the cross section of the coated superalloys as a function of distance from the coating-substrate interface are shown in Fig. 3. The microhardness was measured by a Leitz (Wetzlar, Germany) Hardness Tester Miniload 2, fitted with a Vickers pyramidal diamond indenter. A 15 g (147.1 mN) load was used for penetration and the hardness value was calculated from the relation $Hv = 1854.4 \times F/d^2$ (where F is load in grams and d is the mean penetrated diameter in μm). The microhardness of the substrates and coating was found to be in the range of 315-353 and 850-900 HV, respectively. Standard deviations of the hardness of the coating deposited on the two Ni-base superalloys were found to be in the range of 14.6-20.4 Hv. Two very interesting observations were made after detailed examination of the microhardness profiles. First, both the substrates near the coating interface have shown higher hardness values compared with the core substrates. The reason for this increased hardness values near the coating-substrate interface is attributed to the work hardening effect of sandblasting on the substrate before the coating process as observed by Sundararajan et al. (Ref 13). This increase in hardness is also contributed by the high speed impact of the coating droplets during HVOF spraying as reported by Hidalgo et al. (Ref 14). The second interesting observation is the microhardness of the coatings was found to be much higher than the substrate superalloys. The higher hardness values of the coatings in comparison to the substrate alloys may be due to the high density and cohesive strength of the individual splats as a result of the high impact velocity of the coating particles as suggested by Verdon et al. (Ref 15). Further, some difference in the hardness values of the coating, along the cross section on a particular substrate, has also been noticed. This difference in hardness values of the coatings is due to the presence of porosity, unmelted, melted, and partially melted particles, and oxide inclusions in the coating. The measured values of microhardness of HVOF coating under study are found to be in good agreement with the findings of Vuoristo et al. (Ref 16).

3.3 X-ray Diffraction Analysis

The XRD patterns of the Cr_3C_2-NiCr powder and HVOF sprayed Cr_3C_2-NiCr coatings (Fig. 4) show that powder has main phases of γ-Ni solid solution and Cr_3C_2, whereas coated alloys have a γ-Ni solid solution as the principal phase along with very low intensity peaks of Cr_7C_3 and Cr_2O_3 phases. Dur-

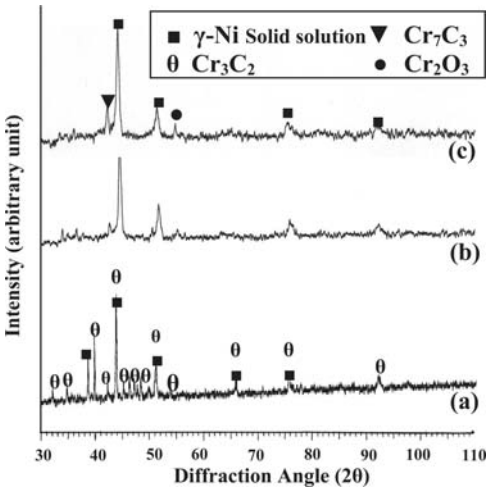

Fig. 4 (a) XRD for the Cr_3C_2-NiCr powder, (b) as-sprayed Cr_3C_2-NiCr coatings on Superni 75, (c) as-sprayed Cr_3C_2-NiCr coatings on Superni 601

ing spraying in the HVOF process, decarburization of Cr_3C_2 might have occurred to form a Cr_7C_3 phase in the coating as has been reported in the literature (Ref 16). Formation of phases in the HVOF sprayed Cr_3C_2-NiCr coating/powder similar to the current study were reported by Vuoristo et al. (Ref 16). The presence of a low intensity peak of Cr_2O_3 indicates that some limited oxidation have occurred at the surface of in-flight particles or at the coating surface, before the deposition of the next layer. Similar findings of formations of oxides in the HVOF coatings have also been reported by Dent et al. (Ref 17).

3.4 Surface and Cross-Sectional Microstructures

From the micrographs of the coating shown in Fig. 5 and 6, it can be inferred that the coating has uniform and dense microstructures and exhibits characteristic splatlike, layered morphologies due to the deposition and resolidification of molten or semimolten droplets. The long axis of the impacted splats are oriented parallel to the substrate surface. A limited number of unmelted particles can be observed in the microstructures. The coatings possess some voids and oxide inclusions that are typical characteristics of the HVOF sprayed coatings. No significant difference is observed between the microstructure of the coating deposited on the two different substrates under study. Only two micrographs of the coating each showing surface and cross-section morphologies are shown in Fig. 5 and 6, respectively.

3.5 Scanning Electron Microscopy/ Energy-Dispersive Analysis

SEM/EDAX shown in Fig. 7 indicates the formation of the required composition for HVOF coatings under study. The regions marked 'M' in these micrographs might have formed from the impact of fully molten feedstock droplets. Subsequently, these droplets have solidified at a high cooling rate, which has been proposed by Moreau et al. (Ref 18) to be typically around 10^7 Ks^{-1} for splat solidification. Such a high cooling rate would result in the formation of a microcrystalline structure. These mi-

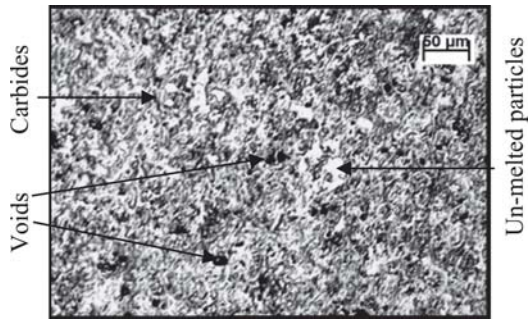

Fig. 5 OM showing surface morphology of as-sprayed Cr_3C_2-NiCr coating

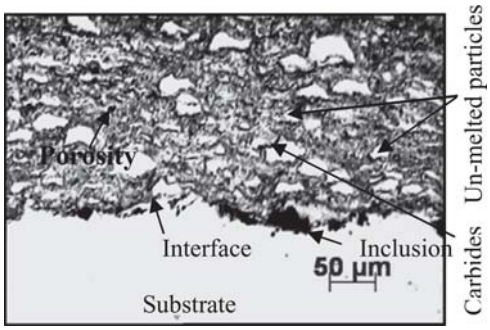

Fig. 6 OM showing cross-sectional microstructure of as-sprayed Cr_3C_2-NiCr coating

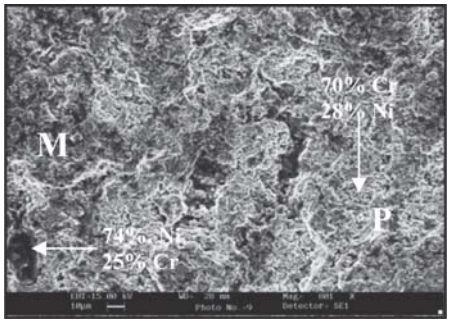

Fig. 7 SEM/EDAX analysis of the HVOF sprayed Cr_3C_2-NiCr coating showing elemental composition (wt.%) at selected points

crocrystalline grains probably solidified directly from the melt by heterogeneous nucleation on preexisting grains of oxide (Ref 17).

EDAX analysis at the cross section of Cr_3C_2-NiCr coated Superni 75 superalloy specimen (Point 1 in Fig. 8) shows the composition almost similar to that of the substrate. At this point, weight percentage of iron is slightly less and nickel is little more than the nominal substrate composition. This indicates the limited diffusion of iron from the substrate to the coating and nickel from the coating to the substrate. The EDAX analysis at Points 2 and 4 showed the contrast phase is the matrix having composition similar to that of the powder. This contrast phase might be a γ-Ni solid solution, a BSE image shows this is the dominating phase of the coating and XRD analysis has detected that the principal phase of the coating is a γ-Ni solid solution. The dark contrast phase might be the Cr-C phase. White phase at Point 3 is found to be nickel-rich splats.

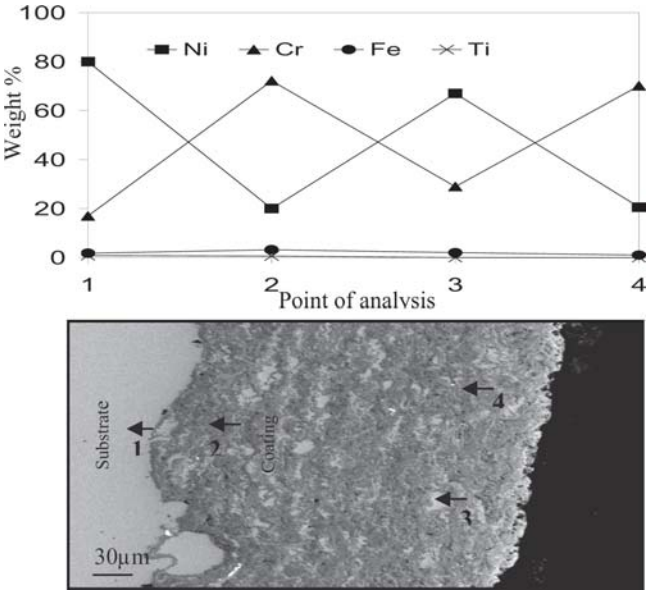

Fig. 8 EDAX analysis at selected point of interest across the cross section of the HVOF sprayed Cr_3C_2-NiCr coating

3.6 Electro Probe Micro Analyzer Analysis

The elemental mappings for the Cr_3C_2-NiCr coating deposited on Superni 75 (Fig. 9) also show that the nickel-rich splats are uniformly distributed in the chromium-rich matrix, which might be a γ-Ni [face-center cubic (fcc)] solid solution as revealed by the XRD analysis. Very small amounts of iron have diffused from the substrate to the coatings mainly through the splat boundaries and formed thin stringers in the form of intersplat lamellae. Inclusions exclusively of aluminum appeared at the coatings-substrate interface, which shows that some amounts of aluminum might have retained in the asperities of the substrate during alumina blasting before the deposition of HVOF coatings.

3.7 Corrosion Kinetics in Molten Salt

Thermogravimetric data for the hot corroded bare and coated superalloy Superni 75 and Superni 601 superalloys has been plotted between weight gains per unit area expressed in mg/cm^2 versus time expressed in number of cycles (Fig. 10). The cumulative weight gain/unit area after 50 cycles of hot corrosion for bare and coated Superni 75 and Superni 601 is shown in Fig. 11. Evidently bare superalloys have gained the higher weight during the course of study. From the weight gain data it can be inferred that Cr_3C_2-NiCr coating deposited on Superni 75 and Superni 601 have provided necessary protection against hot corrosion. The Cr_3C_2-NiCr coating has provided the maximum hot corrosion resistance to Superni 601 superalloy and has been found successful in reducing the weight gain by 70% of that gained by

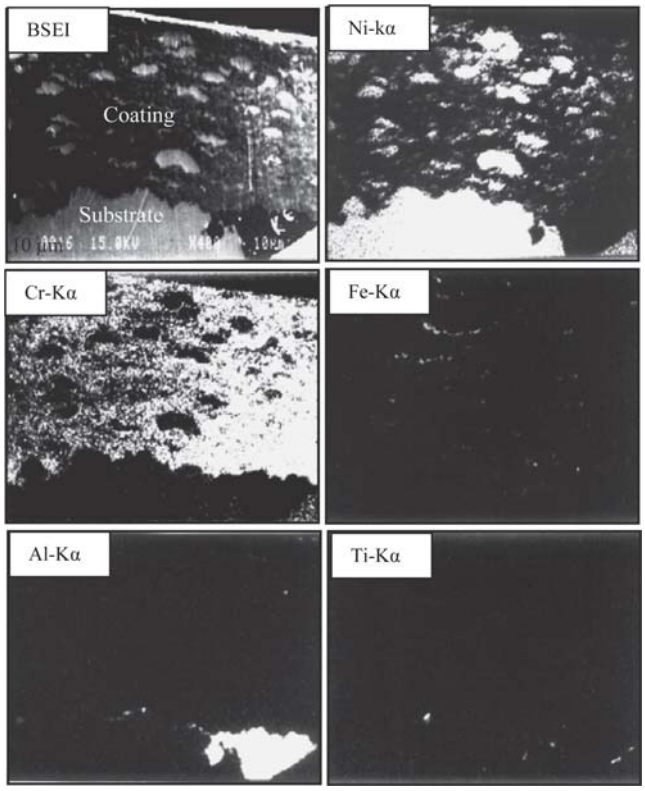

Fig. 9 Composition image (BSEI) and x-ray mapping of the cross section of the as-sprayed Cr_3C_2-NiCr coating on Superni 75 superalloys

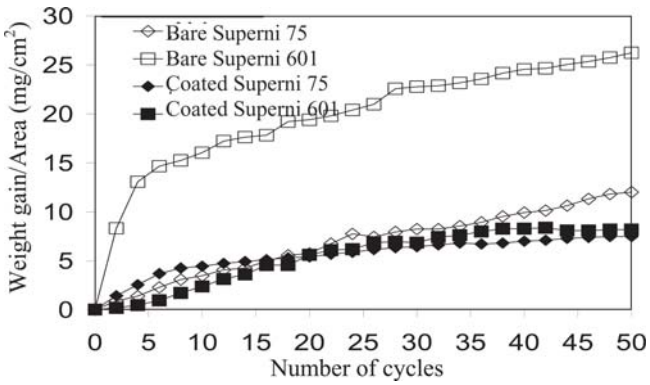

Fig. 10 Weight gain versus number of cycles plot for bare and HVOF Cr_3C_2-NiCr coated superalloys subjected to hot corrosion for 50 cycles in Na2SO4-60%V205 environment at 900 °C

uncoated substrate, whereas coating on Superni 75 superalloy has reduced the weight gain by 40% of that gained by uncoated superalloys.

A fragile scale appeared on the uncoated superalloy during the initial cycles. Subsequently, cracks were developed in the scale and spalling of the scale was observed during the course of study. Some of the scale was seen to be detached from the superalloy surface. The color of the scale, which was brownish gray during early cycles, turned to a dark gray color after some cycles. The Cr_3C_2-NiCr coated superalloy showed minor spallation at the edges and corners during the earlier cycles and the color of the scale, which was dark gray during the first cycle turned to blackish green subsequently.

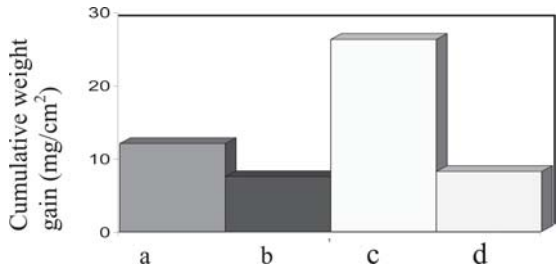

Fig. 11 Cumulative weight after 50 cycles of hot corrosion of bare Cr_3C_2-NiCr coated superalloys (a) bare Superni 75, (b) coated Superni 75, (c) bare Superni 601, (d) coated Superni 601

Further, the weight gain square (mg^2/cm^4) data were plotted as a function of time (number of cycles) as shown in Fig. 12 to establish the rate law for the hot corrosion. The plots show observable deviations from the parabolic rate law for hot corroded Superni 601 superalloy, whereas the fluctuation in data is quite less for bare Superni 75 as well as for coated superalloys. The parabolic rate constants for bare Superni 75 and Superni 601, and for coated Superni 75 and Superni 601 superalloys calculated on the basis of 50 cycles data are found to be 9.716 and 33.586, and 2.997 and 4.707×10^{-10} g^2 cm^{-4} s^{-1}, respectively.

Figure 10 shows that weight gains are relatively higher during the early cycles of the study, and thereafter weight gains are nearly gradual. The initial high oxidation rate of the coated specimens might be attributed to the rapid formation of oxides at the coating splat boundaries and within open pores due to the penetration of the oxidizing species along the splat boundaries/open pores. Once the oxides are formed at places of porosity and splat boundaries and all the accessible internal surfaces have been oxidized, the coating becomes dense and the diffusion of oxidizing species to the internal portions of the coatings gets slowed down and the growth of the oxides becomes limited mainly to the surface of the specimens. This, in turn, will make the weight gain and hence the oxidation rate steady with the progress of exposure time.

The rapid increase in weight gain during the earlier cycles can also be attributed to the possible formation of $NaVO_3$ (m.p. ≈ 610 °C) due to reaction of Na_2SO_4 and V_2O_5 at 900 °C (Ref 19). This $NaVO_3$ serves as an oxygen carrier, which will lead to the rapid oxidation of the coatings as well as bare superalloy to form the protective oxide scale. Slower increase in weight gain during the subsequent cycles is probably due to the growth of oxides, and simultaneously dissolution of Cr_2O_3 in the molten salt is due to the reaction of $Cr_2O_3 + 4NaVO_3 + 3/2O_2 \rightarrow 2Na_2CrO_4 + 2\ V_2O_5$. This Na_2CrO_4 evaporates as a gas.

XRD and EDAX analyses of the Cr_3C_2-NiCr coated alloys showed the formation of NiO, Cr_2O_3, and $NiCr_2O_4$, as the oxide phases on the surface of hot corroded superalloys.

4. Conclusions

Cr_3C_2-NiCr coating has been successfully sprayed by the HVOF process on a Ni-base superalloy with porosity less than

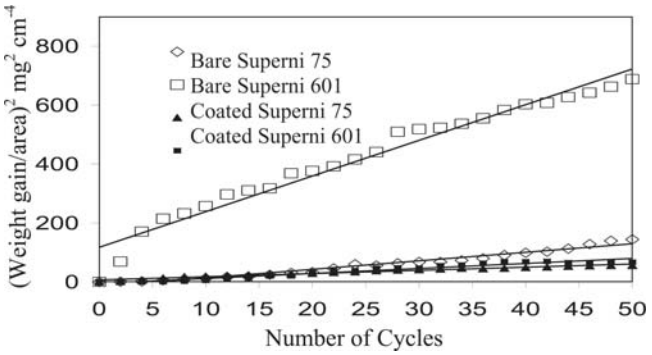

Fig. 12 (Weight gain/area) ^{2} versus number of cycles plot for bare and HVOF Cr_3C_2-NiCr coated superalloys subjected to hot corrosion for 50 cycles in Na_2SO_4-60%V_2O_5 environment at 900 °C

1.5% and microhardness values in the range of 750-930 Hv. The microstructure of the as-sprayed coating has a Ni-base fcc structure as the principal phase with low intensity peaks of Cr_7C_3 and Cr_2O_3 phases. During spraying, decarburization of Cr_3C_2 that is present in the powder might have occurred to form Cr_7C_3 phase in the coating.

The Cr_3C_2-NiCr coating is resistant to hot corrosion in the given molten salt environment at 900 °C, which has been attributed to the formation of oxides of nickel and chromium, and spinels of nickel-chromium. The coating has provided the higher resistance to Superni 601 as compared with Superni 75, and has successfully reduced the weight gain by 70% of that gained by uncoated substrate.

References

1. T.S. Sidhu, S. Prakash, and R.D. Agrawal, State of the Art of HVOF Coating Investigation—A Review, *Mar. Technol. Soc. J.,* 2005, **39**(2), p 55-66
2. N. Eliaz, G. Shemesh, and R.M. Latanision, Hot Corrosion in Gas Turbine Components, *Eng. Fail. Anal.,* 2002, **9,** p 31-43
3. Y.S. Hwang and R.A. Rapp, Thermochemistry and Solubilities of Oxides in Sodium Sulfate-Vanadate Solutions, *Corrosion,* 1989, **45,** p 933-937
4. S.N. Tiwari, "Investigations on Hot Corrosion of Some Fe-, Ni- and Co-Base Superalloy in Na2SO4-V2O5 Environment under Cyclic Conditions," Ph. D. Thesis, Met. Mat. Eng. Dept., University of Roorkee, Roorkee, India, 1997
5. B.Q. Wang and K. Luer, The erosion-oxidation behavior of HVOF Cr_3C_2-NiCr Cermet Coating, *Wear,* 1994, **174,** p 177-185
6. T.S. Sidhu, S. Prakash, and R.D. Agrawal, Characterisation of NiCr Wire Coating on Ni- and Fe- Based Superalloy by HVOF Process, *Surf. Coat. Technol.,* 2006, **200,** p 5542-5549
7. T.S. Sidhu, S. Prakash, and R.D. Agrawal, Characterisation of HVOF sprayed NiCrBSi Coatings on Ni- and Fe- Based Superalloys and Evaluation of Cyclic Oxidation Behaviour of Some Ni-Based Superalloys in Molten Salt Environment, *Thin Solid Films,* 2006, **515,** p 95-105
8. T.S. Sidhu, S. Prakash, and R.D. Agrawal, Hot Corrosion Behaviour of HVOF-sprayed NiCrBSi Coatings on Ni- and Fe-Based Superalloys in Na_2SO_4-V_2O_5 Environment at 900 °C, *Acta Mater.,* 2006, **54,** p 773-784
9. W.-M. Zhao, Y. Wang, T. Han, K.-Y. Wu, and J. Xue, Electrochemical Evaluation of Corrosion Resistance of NiCrBSi Coatings Deposited by HVOF, *Surf. Coat. Technol.,* 2004, **183,** p 118-125
10. "Standard Test Method for Apparent Porosity in Cemented Carbides," B276-05, *Annual Book of ASTM Standards,* ASTM
11. J.M. Guilemany, J. Fernandez, J. Delgado, A.V. Benedetti, and F. Climent, Effects of Thickness Coating on the Electrochemical Behaviour of Thermal Spray Cr_3C_2-NiCr Coatings, *Surf. Coat. Technol.,* 2002, **153**(2-3), p 107-113
12. P.H. Suegama, C.S. Fugivara, A.V. Benedetti, J. Fernandez, J. Delgado, and J.M. Guilemany, Electrochemical Behaviour of Thermally Sprayed Cr3C2-NiCr Coatings in 0.5 M H2SO4 Media, *J. Appl. Chem.,* 2002, **32,** p 1287-1295
13. T. Sundararajan, S. Kuroda, and F. Abe, Steam Oxidation Studies on 50Ni-50Cr HVOF Coatings on 9Cr-1Mo Steel: Change in Structure and Morphology Across the Coating/Substrate Interface, *Mater. Trans.,* 2004, **45**(4), p 1299-1305
14. V.H. Hidalgo, J.B. Varela, J.M. Calle, and A.C. Menendez, Characterisation of NiCr Flame and Plasma Sprayed Coatings for Use in High Temperature Regions of Boilers, *Surface Eng.,* 2000, **16**(2), p 137-142
15. C. Verdon, A. Karimi, and J.-L. Martin, A Study of High Velocity Oxy-Fuel Thermally Sprayed Tungsten Carbide Based Coatings. Part 1: Microstructures, *Mater. Sci. Eng. A,* 1998, **246,** p 11-14
16. P. Vuoristo, K. Niemi, A. Makela, and T. Mantyla, Abrasion and Erosion Wear Resistance of Cr3C2-NiCr Coatings Prepared by Plasma, Detonation and High-Velocity Oxyfuel Spraying, *Proc. 7th National Thermal Spray Conf.,* June 20-24, 1994 (Boston, MA), p 121-126
17. A.H. Dent, A.J. Horlock, D.G. McCartney, and S.J. Harris, Microstructural Characterisation of a Ni-Cr-B-C Based Alloy Coating Produced by High Velocity Oxy-Fuel Thermal Spraying, *Surf. Coat. Technol.,* 2001, **139,** p 244-250
18. C. Moreau, P. Cielo, M. Lamontagne, S. Dallaire, J.C. Krapez, and M. Vardelle, Temperature Evolution of Plasma-Sprayed Niobium Particles Impacting on a Substrate, *Surf. Coat. Technol.,* 1991, **46,** p 173-181
19. G.A. Kolta, I.F. Hewaidy, and N.S. Felix, Reactions Between Sodium Sulphate and Vanadium Pentoxide, *Thermochim. Acta,* 1972, **4,** p 151-164